Proceedings of the 5th International Symposium on Steel Science (ISSS 2017)
Nov. 13-16, 2017, Kyoto, Japan: The Iron and Steel Institute of Japan

Crack formation and propagation mechanism in the punching process of hot-rolled high tensile strength steel sheet

Kazuhiko Yamazaki[1*], Takehiro Okano[2], Chikara Inoue[2], Sota Goto[1], Takeshi Yokota[1], Shinsuke Suzuki[3]

[1] JFE Steel Corporation, 1-1 Minamiwataridacho Kawasaki Kanagawa 210-0855, Japan
[2] Graduate School of Fundamental Science and Engineering, Waseda University, 3-4-1 Okubo, Shinjuku, Tokyo 169-8555, Japan
[3] Faculty of Fundamental Science and Engineering, Waseda University, 3-4-1 Okubo, Shinjuku, Tokyo 169-8555, Japan

Abstract: Applying high tensile strength steel to automotive parts, generation of crack during punching process may become a problem. However, crack formation and propagation mechanism in high tensile strength steel sheets are still uncertain. In this research, influences of microstructure and inclusions in 780 MPa-grade hot-rolled high tensile strength C-Mn steel sheets on crack formation and propagation behaviour during punching process were investigated. Punching test using 20 mmΦ punch was carried out. Crack length and number of cracks were measured and counted by an optical microscope. Afterward, crystal orientation mapping around the crack were obtained by electron backscatter diffraction (EBSD). Additionally, interrupted punching test was conducted. Voids, which were generated in the deformation zone, were observed by field emission scanning electron microscope (FE-SEM). Afterward, element mapping around the void were obtained by electron probe micro analyzer (EPMA). From these results, following tendencies were found. Initiation of voids was at the interface of ferrite matrix and inclusion/precipitation, and interface of ferrite matrix and secondary hard phases such as pearlite. Propagation of cracks was into the ferrite matrix by cleavage. The cracks tend to cause transgranular brittle fracture. From finite element analysis (FEA) and calculation of cleavage strength, critical size of inclusion/precipitation for crack occurrence could be discussed.

1. INTRODUCTION

High tensile strength steel sheets are applied to automotive parts to reduce vehicle weight while ensuring the rigidity of the vehicle body during collision. However, there is a problem that punching process causes more cracks in punched surface on high tensile strength steel sheets than on mild steel sheets [1]. High roughness in punched surface has negative influences on stretch-flange formability [1] and fatigue property [2] so that the crack occurrence in punching process may deteriorates both properties. Thus, suppressing the crack in punching process is important.

The microstructure of steel sheets has been more complicated year by year for the strength of steels [3]. Accordingly, the steel sheets containing secondary phase such as pearlite and martensite are mainly applied to automotive parts [4, 5]. However, there are few studies about effect of microstructure on cracks in the punching process.

In this study, the microstructure around the voids and cracks in punching process was investigated using FE-SEM, EPMA and EBSD analysis to clarify the initiation of the cracks. Afterward, crack propagation mechanism in the punching process were discussed by using FEA method.

2. EXPERIMENTAL PROCEDURES

2.1. Specimen preparation

Hot-rolled 780 MPa-grade high tensile strength C-Mn steel sheets (thickness of 2.6 mm), which consist of ferrite-pearlite (FP) and ferrite-cementite (FC), were prepared. Figure 1 shows the FE-SEM photos of each steel. Pearlite in FP steel showed island shape and dispersed randomly in the ferrite

* Corresponding author. E-mail: k-yamazaki@jfe-steel.co.jp, telephone: +81 44 322 6141.

Table 1. Mechanical properties of steels. JIS No.5 specimen (1.0 mm^t), parallel to RD direction.

Steels	YS (MPa)	TS (MPa)	U.El (%)	T.El (%)
FP	693	798	8.9	15.2
FC	688	778	8.2	15.7

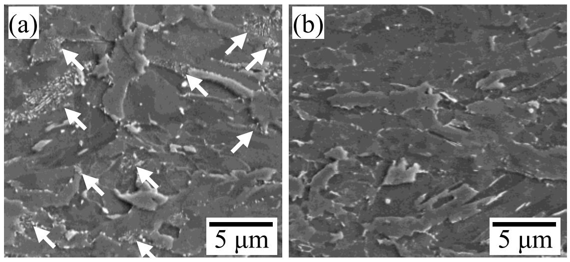

Fig 1. FE-SEM photos (RD direction, nital etchng) of (a) FP steel, (b) FC steel. Pearlite is shown by arrows.

matrix. FC steel showed fine cementite in the ferrite matrix with absence of pearlite. Table 1 shows 0.2% yield strength (YS), tensile strength (TS), uniform elongation (U.El), and total elongation (T.El) of the steels. Center segregation could be the crack initiation site because of its higher hardness than matrix [6]. Therefore, both steels were grinded to 1.0 mm thickness to remove center segregation area in order to clearly observe the effects of microstructure and inclusion/precipitation on punching process.

2.2. Microstructure observation

The pearlite volume fraction and its size, and inclusion size were measured by using FE-SEM photos with magnification of 1500. The pearlite and inclusion/precipitation sizes were defined by the average diameter equivalent to a circle from the FE-SEM photos. The number density of inclusion/precipitation of over 0.5 µm in diameter equivalent to a circle were calculated by using FE-SEM photos with magnification of 1500. Total area of 0.25 mm^2 were observed. The details of the microstructures of the steels were investigated by using an FE-SEM equipped with EBSD detector. The ferrite size was defined by the average diameter equivalent to a circle from the average grain area surrounding the boundaries with misorientation angle of 15° or more.

2.3. Interrupted punching tests

Interrupted punching tests (stroke: 0.5 mm) were conducted with both steels. These tests were carried out with the ratio of clearance between punch (20.0 mmΦ) and die (20.4 mmΦ) to thickness of 20% at punching velocity of 1 mm/min.

Voids, which were initiated in the deformation zone, were observed by an FE-SEM. Afterward, element mapping around the void in the surface parallel to the rolling direction was obtained by EPMA. Microstructure observation with 3% nital etching was carried out for the same area as the void observation.

2.4. Punching tests

Punching tests were conducted with both steels. These tests were carried out with the ratio of clearance to thickness of 20% at punching velocity of 1 mm/min.

Crack length (≥ 10 µm) and number of cracks were measured and counted by an optical microscope (OM). Fifty specimens for each steel sheet were prepared for the observation. Crack length were measured and counted on the cross section of punched edge parallel and perpendicular to the rolling direction. In total, 100 cross sections of punched edge were observed in each steels. Crack length was defined as horizontal length on the cross section around the crack as shown in Fig. 2.

Punched edge surface observation was carried out by using an FE-SEM to distinguish fracture mode. Crystal orientation mapping around the crack was obtained by EBSD.

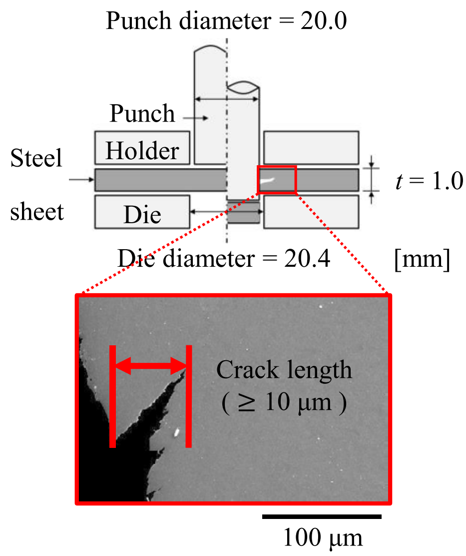

Fig 2. Punching test and crack length measurement.

Table 2. Characteristics of microstructure of steels.

Steels	Ferrite grain diameter (μm)	Pearlite grain diameter (μm)	Pearlite volume fraction (%)	Inclusion/ precipitation diameter (μm)
FP	2.0	1.9	7	1.1
FC	2.1	-	-	1.3

3. RESULTS AND DISCUSSION

3.1. Microstructure of steels

Table 2 shows the characteristics of microstructure of each steels. Figure 3 shows the distribution of inclusion/precipitation sizes in both steels. Inclusion diameter of 3.5 μm and over were all TiN. Average ferrite grain sizes and the average sizes and distribution of inclusions were similar in both steels.

3.2. Interrupt punching test

In the interrupted punching tests, voids, which initiated in the deformation zone, were observed by FE-SEM. Voids initiated at the interface of the ferrite matrix and inclusions/precipitation in the both steel. In FP steel, initiation of void in pearlite was also observed. Figure 4 shows FE-SEM photos and EPMA mappings of Ti, N and S on the cross section around the void in the FP steel. This result shows that voids are initiated at the interface of ferrite matrix and pearlite, and ferrite matrix and inclusion/precipitation such as TiN and TiS.

3.3. Punching test

Relationship between the number of cracks and crack length in the FP and FC steels are shown in Fig. 5. The total numbers of 154 cracks were observed in FP steel and the total number of 50 cracks were observed in FC steel. Number of crack in FP steel showed three times higher compared to FC steel. Assuming that the cracks were initiated from the void, since coarse pearlite, which can function as void initiation site, were dispersed in FP steel, the number of cracks of FP steel was higher than that of FC steel.

Figure 6 shows the FE-SEM photos of punched edge surface in FC steel sheets and the cross section IPF map of the crack. The surface near the crack showed brittle fracture surface and the surface away from the crack showed ductile fracture surface with dimples. Cross section IPF map of the crack shows that the crack propagation occurred parallel to {001} plane of ferrite matrix, which indicates that transgranular cleavage fracture were occurred.

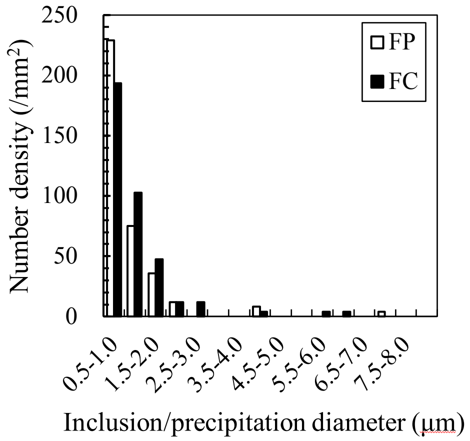

Fig 3. Inclusion distribution of each steels.

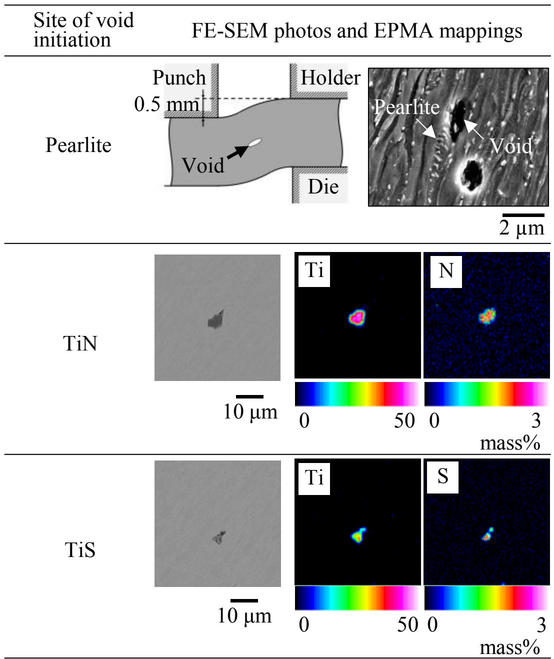

Fig 4. FE-SEM photos and EPMA mappings of Ti, N and S around the void in FP steel sheets in interrupt punching test.

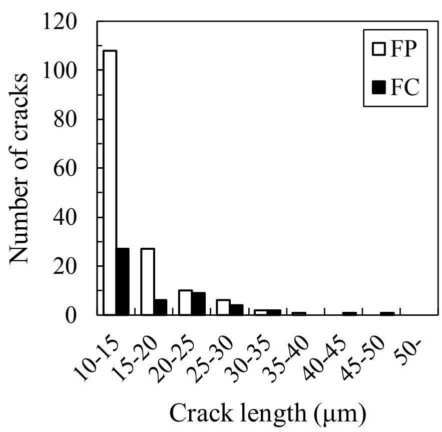

Fig 5. Relationship between crack length and number of cracks in punching test.

3.4. Finite element analysis of punching test

A FEA of the punching test was conducted by using ABAQUS Ver. 6. 6. 2 to clarify the reason for crack occurrence in the punching test. Figure 7 shows the contour figures of the von Mises stress just before fracture of FC steel. The maximum principal stress (σ_I) was calculated as 1037 MPa in the center of fractured edge while equivalent plastic strain was 1.20 in the same position. Cleavage strength (σ_C) can be expressed as following equation [7].

$$\sigma_C = \sqrt{\frac{4E\gamma}{\pi(1-\nu^2)d_I} - \frac{k^2 d_\alpha}{8\pi^2 {d_I}^2} - \frac{k\sqrt{d_\alpha}}{2\sqrt{2}\pi d_I}} \quad (1)$$

where E is Young's modulus, γ is the free energy of the boundary, ν is Poisson's ratio, d_α is ferrite grain diameter, d_I is inclusion/precipitation diameter, k is coefficient of the Hall-Petch equation.

When σ_I that is calculated by FEA exceeded σ_c which is calculated from Eq. 1, crack may possibly occur during the punching process. Therefore, by combining FEA and Eq. 1, critical size of inclusion/precipitation for crack occurrence can be estimated.

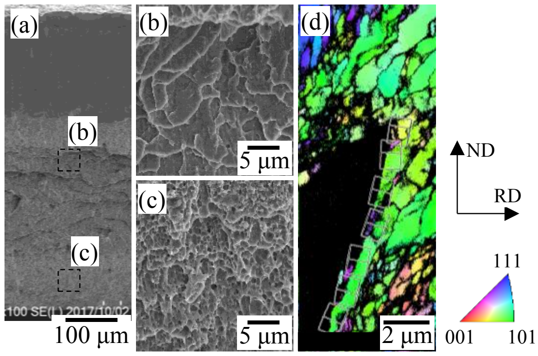

Fig 6. FE-SEM photos of (a) punched edge surface, (b) brittle fracture surface near the crack, and (c) ductile fracture surface away from a crack in FP steel. (d) Cross section IPF map of the crack in FP steel.

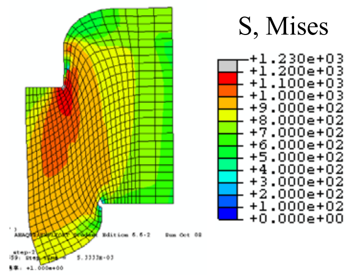

Fig 7. Contour figures of the von Mises stress just before fracture in punching test of FC steel.

4. CONCLUSION

In this study, crack formation and propagation mechanism in the punching process were investigated using 780 MPa-grade high tensile strength C-Mn steels which consist of ferrite-pearlite and ferrite-cementite. The following results were obtained.

1. In the punching process, voids tend to initiate at ferrite matrix and inclusion/precipitation (TiN, TiS) and also ferrite matrix and pearlite interface.
2. The number of cracks was three times higher in FP steel compared with FC steel. Since the number density and size of inclusion/precipitation in both steels were similar, crack formations were considered to be promoted by pearlite.
3. The crack propagation occurred parallel to {001} plane of ferrite matrix, which indicates that transgranular brittle fracture were occurred during punching process.
4. From FEA results and calculation of cleavage strength from Eq. 1, critical size of inclusion/precipitation for crack occurrence can be estimated.

REFERENCES

[1] E. Iizuka, T. Hira and A. Yoshitake: Jpn. Soc. Technol. Plasticity, 46 (2005), 625.
[2] K. Tomita, T. Shiozaki, T. Urabe and K. Osawa: Tetsu-to-Hagané, 87 (2001), 557.
[3] K. Nakaoka: Tetsu-to-Hagané, 68 (1982), 1159.
[4] R. Mizuno, H. Matsuda, Y. Funakawa and Y. Tanaka: Tetsu-to-Hagané, 96 (2010), 414.
[5] K. Hasegawa, Y. Toji, H. Minami, H. Ikeda, T. Morikawa and K. Higashida: Tetsu-to-Hagané, 98 (2012), 320.
[6] K. Sakumoto, K. Yamazaki, T. Kobayashi and S. Suzuki: Key Eng. Mater., 622-623 (2014), 1075.
[7] N. J. Petch: Acta Metall, 34 (1986) 7, 1387.